# Size-Dependent Relaxation Properties of Monodisperse Magnetite Nanoparticles Measured Over Seven Decades of Frequency by AC Susceptometry

R. Matthew Ferguson[1], Amit P. Khandhar[1], Christian Jonasson[2], Jakob Blomgren[2], Christer Johansson[2], and Kannan M. Krishnan[1]

[1]Department of Materials Science, University of Washington, Seattle, WA 98195 USA
[2]Acreo AB, SE 400 16 Göteborg, Sweden

**Magnetic relaxation is exploited in innovative biomedical applications of magnetic particles such as magnetic particle imaging (MPI), magnetic fluid hyperthermia, and bio-sensing. Relaxation behavior should be optimized to achieve high performance imaging, efficient heating, and good SNR in bio-sensing. Using two AC susceptometers with overlapping frequency ranges, we have measured the relaxation behavior of a series of monodisperse magnetic particles and demonstrated that this approach is an effective way to probe particle relaxation characteristics from a few Hz to 10 MHz, the frequencies relevant for MPI, hyperthermia, and sensing.**

***Index Terms*—AC susceptometry, magnetic particle imaging, magnetic particles, magnetization reversal.**

## I. Introduction

MAGNETIC relaxation is exploited in innovative biomedical applications of magnetic particles such as magnetic particle imaging (MPI), magnetic fluid hyperthermia, and biosensing [1]. Magnetic relaxation describes the physical phenomena governing how magnetic particles reverse their magnetic moment, as a function of time, in response to a changing applied field. For particles in solution, the relaxation time is influenced by particle size and local environment; by controlling size, relaxation can be tuned for the chosen application.

For MPI [2], [3] and hyperthermia [4], magnetic relaxation is used to generate an image or heat, respectively. In MPI, particle relaxation is tuned for a given imaging system, which operates at a fixed frequency, to minimize the relaxation time, maximize the time rate change of magnetic moment, dm/dt, and thereby generate a strong inductive response in the imaging system. In hyperthermia, on the other hand, relaxation is tuned so that the magnetization is out-of-phase with the driving field so as to maximize heat deposition in the particle. In both cases, broadband relaxation measurements, which provide a direct measurement of the particle response to a driving field over a wide frequency range, are valuable for particle optimization. Néel relaxation studies, which probe magnetic crystal properties by measuring the internal rotation of the magnetic moment, reveal information about magnetic anisotropy, relaxation rates, and core-size distribution that is useful for optimizing performance, for example in MPI and hyperthermia.

In contrast to Néel relaxation studies, where internal magnetic properties dominate, Brownian relaxation studies measure in large extent the properties around the particles, for instance their hydrodynamic size and interaction with surrounding liquid or other substances. By probing properties external to the magnetic particle, Brownian relaxation measurements provide a method for bio-sensing that can be used to detect, isolate, or quantify changes in particle hydrodynamic size or local environment [5]–[7], for example due to binding of target moieties to a receptor-conjugated nanoparticle [8]. For such applications, relaxation time is monitored to detect changes in hydrodynamic size that occur when the target binds to a complementary receptor at the nanoparticle's surface. The larger hydrodynamic size of the coupled particle system slows its relaxation time.

The range of frequencies relevant for magnetic relaxation measurements extends from a few Hz, the slowest Brownian relaxation time of magnetically blocked particles, to hundreds of MHz for Neel relaxation in small, thermally activated particles (Fig. 1). (At even higher frequencies, e.g. the GHz range, it is possible to use AC susceptometry to measure ferro- and ferrimagnetic resonance within the magnetic crystals [9].) A set of two AC susceptibility systems designed by Acreo AB,

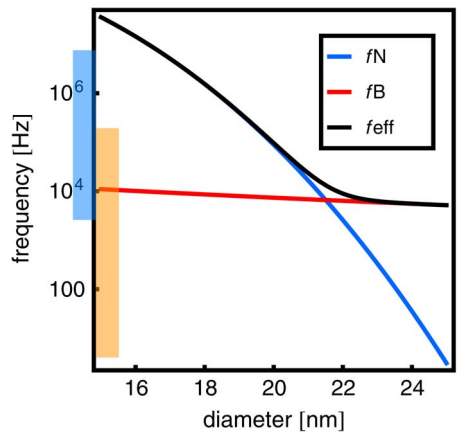


Fig. 1. Relaxation frequency $(1/(2\pi\tau))$ calculated according to (3), (4), and (5). For calculations, the hydrodynamic layer thickness, $\delta$, was assumed to be 10 nm, and the magnetocrystalline anisotropy, $K$, was the bulk value, $1.1 \times 10^4$ $\mathrm{Jm}^{-3}$, for magnetite at 298 K. The blue shaded area represents the frequency range probed by the Acreo HF AC Susceptometer, and the orange shaded area the frequency range probed by the DynoMag system.

Manuscript received November 02, 2012; accepted January 04, 2013. Date of current version July 15, 2013. Corresponding author: K. M. Krishnan (e-mail: kannanmk@uw.edu).

Color versions of one or more of the figures in this paper are available online at http://ieeexplore.ieee.org.

Digital Object Identifier 10.1109/TMAG.2013.2239621

with overlapping frequency ranges covering from a few Hz to 10 MHz (the DynoMag and HF AC Susceptometer [8]), can probe the full range of relaxation times relevant for bio-sensing (Hz–kHz), MPI (25 kHz), and hyperthermia (hundreds of kHz). Furthermore, such a combination of susceptometer systems enables relaxation-time analysis of nanoparticle samples in the scientifically interesting transition region between Néel and Brownian relaxation.

In this work, we have used the Acreo systems to measure relaxations of a series of magnetite nanoparticles with narrow size distributions. The particles featured increasing size and we observed a transition in their relaxation behavior, from Brownian-dominated relaxation for the largest particles, to Néel-dominated relaxation for the smallest particles, with a mix of both behaviors in an intermediate sample.

## II. Methods

### A. Synthesis, Preparation, and Physical Characterization of Nanoparticles

Nanoparticles were prepared in organic solvents and subsequently dispersed in aqueous solution following previously published methods [4]. Measurements of M(H) were performed in a LakeShore VSM up to 1 T, at room temperature. Magnetic size distributions were determined by the Chantrell method [10], assuming a log-normal distribution function of the form

$$g(r_c) = \frac{1}{\sigma * r_c * \sqrt{2 * \pi}} \exp - \frac{\ln\left(\frac{r_c}{r_0}\right)^2}{2 * \sigma^2} \tag{1}$$

where $r_c$ is the particle magnetic core radius, $\sigma$ is the distribution shape parameter, and $r_0$ the median magnetic core radius.

Bright field TEM measurements were performed using an FEI Tecnai TEM. Size was measured by counting particles using the free Particle Size Analyzer (PSA, version:r12) macro package in ImageJ.[1] Histograms were fitted to a log normal distribution of the form used in (1).

### B. Single-Core Debye AC Susceptibility Model

A single-core Debye AC susceptibility model was used to analyze relaxation data. Particles were assumed to have single-domain cores so that the AC susceptibility is given by

$$\chi(\omega) = C \int \frac{r_C^6}{(1 + j\omega\tau_{eff}(r_C, \delta)} f(r_C) dr_C + \chi_{high} \tag{2}$$

where $f(r_C)$ is the magnetic core size distribution (particle number distribution), which is assumed to be log-normal as in (1), with a median magnetic core radius, $r_C$, and size width distribution parameter, $\sigma$; $C$ is a coefficient that includes temperature, particle number density, and intrinsic particle magnetization; $\omega = 2\pi f$, $f$ is the excitation frequency, and $\chi_{high}$ is the real component of the high frequency susceptibility. The effective relaxation time, $\tau_{eff}$, is defined by

$$\tau_{eff} = \frac{\tau_B \tau_N}{\tau_B + \tau_N}. \tag{3}$$

[1]http://code.google.com/p/psa-macro/

The Brownian relaxation time, $\tau_B$, is

$$\tau_B = \frac{3V_H\eta}{k_bT} = \frac{4\pi r_H^3 \eta}{k_bT} \tag{4}$$

where $V_H$ is the hydrodynamic volume and $r_H$ the hydrodynamic radius, the Boltzmann constant, $k_b$, is $1.38 \times 10^{-23}$ m$^2$ kg s$^{-1}$ K$^{-1}$, the fluid viscosity, $\eta$, was $0.9 \cdot 10^{-3}$ Pa s, and the measurement temperature, $T$, was 298 K. The Néel relaxation time, $\tau_N$, is given by

$$\tau_N = \tau_0 e^{\frac{KV_c}{k_bT}} \tag{5}$$

where the anisotropy constant, $K$, was $1.1 \times 10^4$ J m$^{-3}$, the bulk value for magnetite. $V_c$ is the particle's magnetic core volume, and the attempt time, $\tau_0$, was $10^{-10}$ s. The hydrodynamic radius, $r_H$, is related to the magnetic core radius, $r_c$, by $r_H = r_c + \delta$, where $\delta$ is the thickness of the hydrodynamic surface layer.

### C. Relaxation Measurements

Nanoparticle samples were suspended in water. For each sample, 200 $\mu$L of suspension was measured in a sample cuvette and inserted into the Acreo DynoMag system and subsequently the HF AC Susceptometer. Magnetic field amplitudes during measurement were 0.5 mT/$\mu_0$ (max) in the DynoMag system and 0.03 mT/$\mu_0$ (max) in the HF system and the measurement temperature was 298 K.

## III. Results and Discussion

We evaluated magnetic relaxations of a series of magnetite nanoparticles synthesized in our labs, using the two AC susceptibility systems designed by Acreo AB: the DynoMag [8] and HF AC Susceptometer [11]. With increasing nanoparticle size, we observed an increase in relaxation time that corresponded to a transition from Néel to Brownian relaxation [Fig. 2(a)–(c)]. The real ($\chi'$), and imaginary ($\chi''$) parts of (2) are plotted in the figure. From (2), the $\chi''$ peak in frequency mirrors the change in the mean relaxation time. We observed the relaxation frequency to decrease from about 500 kHz for the smallest sample (sample UW1 in Table I), to about 1 kHz for the largest sample (Sample UW3). Sample core radius, $r_c$, for the three samples was determined to be 9.1, 8.8, and 11.9 nm by curve fitting using the single-core susceptibility model and with a surface thickness $\delta = 10$ nm for all samples, which gave the best fitting result. Calculated size distributions are presented in Figs. 2(c)–3, and in Table I. Surface thicknesses of 10 nm are reasonable for the UW particles, which had hydrodynamic radii, $r_H$, of ~15 nm (number-weighted; ~20 nm, volume-weighted) in photon correlation spectroscopy (PCS) measurements (data not shown).

The measured $\chi''$ peak appears broad for samples UW1 and UW2, despite the relatively narrow size-distribution shape parameter determined by fitting to the data. This can be explained by the strong Néel relaxation behavior in the sample and the exponential dependence of the Néel relaxation time with core volume, $V_C$ (5), meaning that even a small size distribution will give a large distribution of Néel relaxation times that is visible in

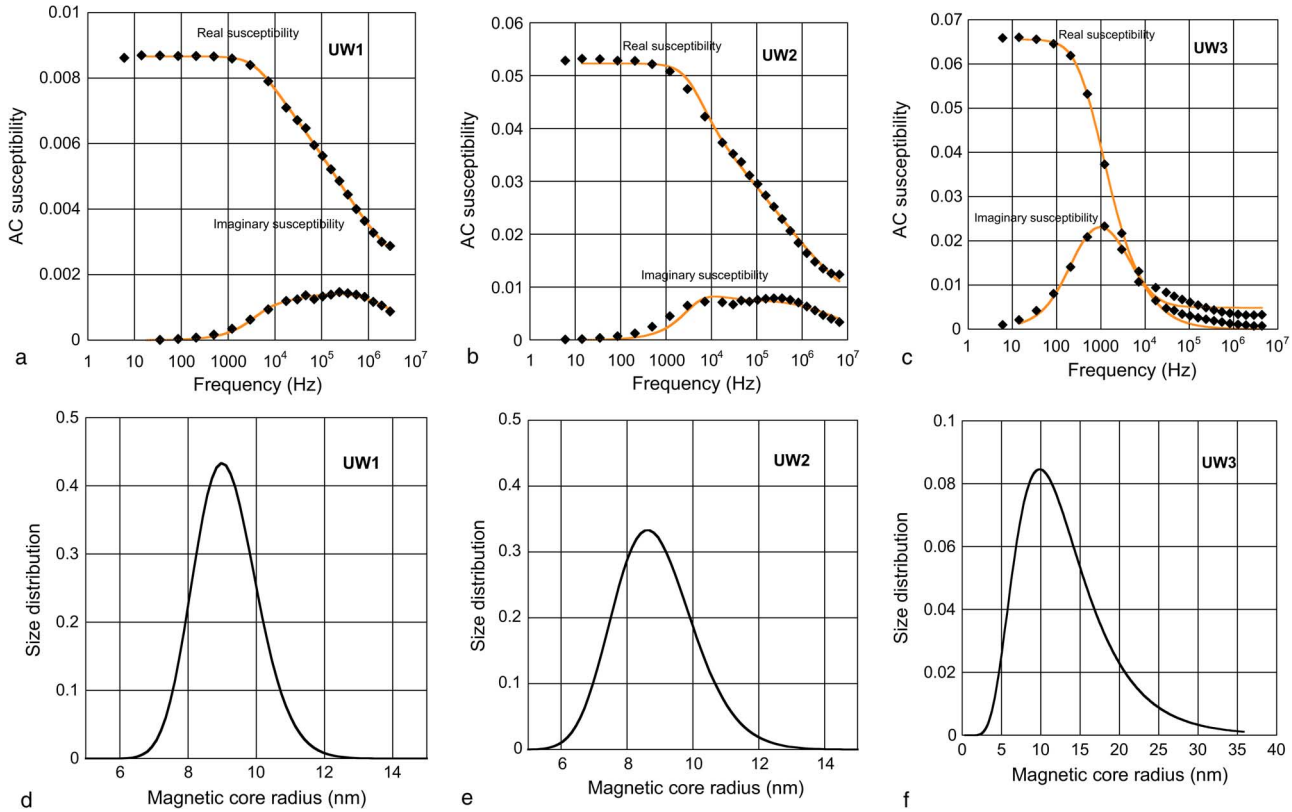


Fig. 2. a–c) Measurements of relaxation by ac susceptibility (filled diamonds) for magnetite nanoparticles listed in Table I. Solid lines are fits to the data using the single-core susceptibility model. d–f) Particle size determined from relaxation measurements, assuming a log-normal distribution as in (1).

TABLE I
MEASURED NANOPARTICLE SIZES

| | median core radius, $r_c$ [nm] ($\sigma$) | | |
|---|---|---|---|
| | M(H) fitting | AC Susceptibility | TEM |
| UW1 | 9.0 (0.19) | 9.1 (0.11) | 10.1 (0.33) |
| UW2 | 10.2 (0.20) | 8.8 (0.15) | 10.7 (0.26) |
| UW3 | 13.4 (0.29) | 11.9 (0.44) | 13.6 (0.22) |

the AC susceptibility versus frequency response. Sample UW2 showed a mix of Néel and Brownian behavior, as evidenced by the appearance of multiple peaks, one at lower frequency (∼10 kHz), due to Brownian relaxation, and a second broad peak at higher frequency (∼0.5 MHz), due to Néel relaxation. Samples like UW1 and UW2 with median diameters at the transition size in Fig. 1 will show a mixture of relaxation mechanisms, given the inevitable presence of a size distribution, albeit narrow, within the sample.

Magnetic core size was also determined by fitting to M(H) measurements of liquid sample suspensions, assuming a log-normal distribution of the form in (1). Fig. 3(a) shows an example M(H) measurement and fit of sample UW3; results for all samples are provided in Table I. Samples UW1 and UW2 had relatively narrow size distributions (0.19 and 0.2, respectively), while again sample UW3 featured a broader distribution (0.29) in keeping with that measured by AC susceptibility.

Particle size was also measured with TEM imaging. Results generally agree with those measured by relaxation and M(H),

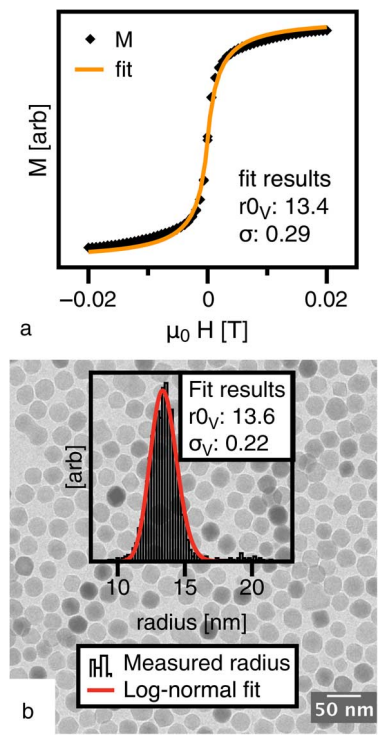


Fig. 3. Size determination of UW3 by a) Chantrell fitting to M(H) data and b) TEM counting. A volume-weighted log-normal distribution as in (1), with median radius, $r0_V$, and distribution shape parameter, $\sigma_V$, was assumed.

though TEM size was slightly larger for each sample. Size measured by TEM is commonly observed to be larger than that determined by M(H) measurements, since TEM measures the

crystal size, whereas M(H) measurements determine the magnetic domain size, which is often slightly smaller than the crystal size due to surface effects. Relaxation measurements, on the other hand, measure magnetic core size when Néel relaxation dominates, but hydrodynamic particle size for Brownian-dominated particles.

It is necessary to determine nanoparticle magnetic relaxation behavior in order to optimize performance for applications in MPI and magnetic fluid hyperthermia. For these applications, depending on the applied field frequency, we are typically interested in nanoparticles with radius between 9 and 13 nm, which lie in the region of transition from thermally activated to magnetically blocked behavior. AC susceptometers can enable unambiguous relaxation measurements over a wide frequency range that incorporates both Néel and Brownian regimes. The AC susceptometers used in this study are based on induction techniques that give higher magnetic resolution and easier sample handling than other methods, for example the Fannin split-toroid method [12]. Finally, relaxation measurements provide critical input for nanoparticle design in a variety of biomedical applications, including our own work in MPI [13], [14] and hyperthermia [4].

## ACKNOWLEDGMENT

This work was supported by NIH/NIBIB grant number R01EB013689.

## REFERENCES

[1] K. M. Krishnan, "Biomedical nanomagnetics: A spin through possibilities in imaging, diagnostics, and therapy," *IEEE Trans. Magn.*, vol. 46, no. 7, pp. 2523–2558, Jul. 2010.

[2] R. M. Ferguson, A. P. Khandhar, and K. M. Krishnan, "Tracer design for magnetic particle imaging (invited)," *J. Appl. Phys.*, vol. 111, no. 7, p. 07B318, 2012.

[3] P. W. Goodwill, A. Tamrazian, L. R. Croft, C. D. Lu, E. M. Johnson, R. Pidaparthi, R. M. Ferguson, A. P. Khandhar, K. M. Krishnan, and S. M. Conolly, "Ferrohydrodynamic relaxometry for magnetic particle imaging," *Appl. Phys. Lett.*, vol. 98, no. 26, pp. 262502–262502, 2011.

[4] A. P. Khandhar, R. M. Ferguson, J. A. Simon, and K. M. Krishnan, "Tailored magnetic nanoparticles for optimizing magnetic fluid hyperthermia," *J. Biomed. Mater. Res. Part A*, vol. 100, no. 3, pp. 728–737, 2012.

[5] A. P. Astalan, F. Ahrentorp, C. Johansson, K. Larsson, and A. Krozer, "Biomolecular reactions studied using changes in Brownian rotation dynamics of magnetic particles," *Biosens. Bioelectron.*, vol. 19, no. 8, pp. 945–951, Mar. 2004.

[6] Y. Bao, A. Pakhomov, and K. Krishnan, "Brownian magnetic relaxation of water-based cobalt nanoparticle ferrofluids," *J. Appl. Phys.*, vol. 99, no. 8, p. 08H107, 2006.

[7] S. Kalele, R. Narain, and K. M. Krishnan, "Probing temperature-sensitive behavior of pNIPAAm-coated iron oxide nanoparticles using frequency-dependent magnetic measurements," *J. Magn. Magn. Mater.*, vol. 321, no. 10, pp. 1377–1380, 2009.

[8] T. Z. N. G. de la Torre, A. Mezger, D. Herthnek, C. Johansson, P. Svedlindh, M. Nilsson, and M. Strømme, "Detection of rolling circle amplified DNA molecules using probe-tagged magnetic nanobeads in a portable AC susceptometer," *Biosens. Bioelectron.*, vol. 29, no. 1, pp. 195–199, Nov. 2011.

[9] P. C. Fannin, T. Relihan, and S. W. Charles, "Investigation of ferromagnetic resonance in magnetic fluids by means of the short-circuited coaxial line technique," *J. Phys. D Appl. Phys.*, vol. 28, no. 10, pp. 2003–2006, Jan. 1999.

[10] R. W. Chantrell, J. Popplewell, and S. W. Charles, "Measurements of particle size distribution parameters in ferrofluids," *IEEE Trans. Magn.*, vol. 14, no. 5, pp. 975–977, 1978.

[11] F. Ahrentorp, A. P. Astalan, C. Jonasson, J. Blomgren, B. Qi, O. T. Mefford, M. Yan, J. Courtois, J. F. Berret, J. Fresnais, O. Sandre, S. Dutz, R. Müller, and C. Johansson, "Sensitive high frequency AC susceptometry in magnetic nanoparticle applications," in *Proc. AIP Conf.*, 2010, vol. 1311, pp. 213–223.

[12] P. Fannin, B. Scaife, and S. Charles, "New technique for measuring the complex susceptibility of ferrofluids," *J. Phys. E: Sci. Instrum.*, vol. 19, no. 3, pp. 238–239, 1986.

[13] P. W. Goodwill, E. U. Saritas, L. R. Croft, T. N. Kim, K. M. Krishnan, D. V. Schaffer, and S. M. Conolly, "X-Space MPI: Magnetic nanoparticles for safe medical imaging," *Adv. Mater.*, vol. 24, pp. 3870–3877, 2012.

[14] R. M. Ferguson, K. R. Minard, A. P. Khandhar, and K. M. Krishnan, "Optimizing magnetite nanoparticles for mass sensitivity in magnetic particle imaging," *Med. Phys.*, vol. 38, no. 3, pp. 1619–1626, Feb. 2011.